PERGAMON

Microelectronics Reliability 42 (2002) 1457–1460

MICROELECTRONICS RELIABILITY

www.elsevier.com/locate/microrel

Simulative prediction of the resistance change due to electromigration induced void evolution

Hajdin Ceric[1] and Siegfried Selberherr

Institute for Microelectronics, TU Vienna, Gusshausstr. 27-29/E360, A-1040 Vienna, Austria

Abstract

We apply a diffuse interface model to the analysis of void evolution with an electron wind and the chemical potential gradient as the main driving forces. Simulations were carried out for voids exposed to high current. Emphasis was put on the influence of the void dynamics on the resistance of interconnect structures. In the case of an interconnect via it was shown that a migrating void exactly follows the current flow, retaining its stability, but due to change of shape and position causes significant fluctuations in interconnect resistance. For the first time the diffuse interface governing equation was solved applying an adaptive finite element scheme with a robust local mesh refinement algorithm.

1. Introduction

One of the most important issues in the reliability study of integrated circuits interconnect lines is electromigration. This phenomena results in the formation and growth of voids which can cause significant fluctuations in interconnect resistance and in the extreme case sever the interconnect line. To accurately simulate interconnect resistance change due to electromigration, tracking the void shape and position is necessary. Simulations of void evolution in linear interconnect began with sharp interface models which showed the insufficiency of sharp interface models [6, 2]. Later, prompted by the complexity of void surfaces, diffuse interface models were introduced [1]. An alternative diffuse interface model based on the double obstacle potential was proposed in [3]. However, all these methods require structured meshes and were applied to simple rectangular interconnect geometries. To reach higher mesh adaptability and appropriate refinement quality for the finite element scheme solving the diffuse interface model, we used a version of recursive local mesh refinement algorithm introduced in [5].

2. Applied diffuse interface model

We assumed unpassivated monocrystal isotropic interconnects where stress phenomena can be neglected. An interconnect is idealized as two-dimensional electrically conducting via which contains initially circular void. For simplicity we also neglect the effects of grain boundaries and lattice diffusion. In this case there are two main forces which influence the shape of the evolving void interface: the chemical potential gradient

[1]Corresponding author. Tel.: +43-1-58801/36032; fax: +43-1-58801/36099.
E-mail address: Ceric@iue.tuwien.ac.at

0026-2714/02/$ - see front matter
PII: S0026-2714(02)00169-5

and electron wind. The first force causes self-diffusion of metal atoms on the void interface and tends to minimize energy which results in circular void shapes. The electron wind force produces asymmetry in the void shape depending on electrical field gradients. In the diffuse interface models void and metal area presented through the order parameter ϕ which takes values $+1$ in the metal area, -1 in the void area and $-1 < \phi < +1$ in the void-metal interface area. The model equations for the void evolving in an unpassivated interconnect line are for the order parameter [3],

$$\frac{\partial \phi}{\partial t} = \frac{2D_s}{\epsilon\pi}\nabla \cdot (\nabla\mu - |e|Z^*\nabla V) \tag{1}$$

$$\mu = \frac{4\Omega\gamma_s}{\epsilon\pi}(f'(\phi) - \epsilon^2\Delta\phi) \tag{2}$$

and for the electrical field

$$\nabla \cdot (\sigma(\phi)\nabla V) = 0 \tag{3}$$

where D_s is the surface diffusivity, μ is the chemical potential, Z^* is the effective valence, e is the charge of an electron, γ_s is the surface energy, Ω is the volume of an atom, $f(\phi)$ is the double obstacle potential as defined in [3], ϵ is a parameter controlling the void-metal interface width and V is the electrical potential. The electrical conductivity was taken to vary linearly from the metal ($\sigma = \sigma_{metal}$) to the void area ($\sigma = 0$) by setting $\sigma = \sigma_{metal}(1+\phi)/2$. The equations (1) and (3) are solved on the two-dimensional polygonal interconnect area T.

3. Numerical implementation

3.1. Finite element scheme

Let $\Lambda_h(t_{n-1})$ be a triangulation of the area T at the discrete time t_{n-1}, and let $\{\phi^{n-1}\}_{i=0}^{N-1}$ be discrete nodal values of order parameter on this triangulation. A finite element based iteration for solving (1) on mesh $\Lambda_h(t_{n-1})$ and evaluating the order parameter at the time $t_n = t_{n-1} + \Delta t$ consists of two steps [4]:

Step 1. For the k^{th} iteration of n^{th} time step the linear system of equations has to be solved:

$$\epsilon\frac{\pi}{2}M_{ii}\phi_i^{n,k} + \Delta t D_s K_{ii}\mu_i^{n,k} = \alpha_i \tag{4}$$

$$M_{ii}\mu_i^{n,k} - \tau\left(\frac{1}{\epsilon}M_{ii} + \epsilon K_{ii}\right)\phi_i^{n,k} = \beta_i, \tag{5}$$

where

$$\alpha_i = \epsilon\frac{\pi}{2}M_{ii}\phi_i^{n-1} - \Delta t D_s \sum_{i\neq j} K_{ij}\mu_j^{n,k-1} \tag{6}$$

$$\beta_i = \tau\epsilon\sum_{i\neq j} K_{ij}\phi_j^{n,k-1} - |e|Z^*M_{ii}V_i^{n-1} \tag{7}$$

for each $i = 0, N-1$ of the nodal values (ϕ_i^n, μ_i^n) of the triangulation T_h. $[M]_{ij}$ and $[K]_{ij}$ are the lumped mass and stiffness matrix, respectively and $\tau = \frac{4\Omega\gamma_s}{\pi}$.

Step 2. All nodal values $\{\phi^n\}_{i=0}^{N-1}$ are projected on $[-1,1]$ by a function

$$\rho(x) = max(-1, min(1, x)). \tag{8}$$

For solving (3) a conventional finite element scheme is applied.

As we will see in the next section, in order to reach appropriate accuracy, schemas for the finite element solving of equation (1) require sequential mesh adaptation in each time step. For the mesh transformation we used a general adaptive algorithm with flexible refinement-coarsening pattern which transforms mesh $\Lambda_h(t_n)$ into mesh $\Lambda_h(t_{n+1})$ according to certain defined condition $COND$.

$$\Psi(\Lambda_h(t_n), COND) = \Lambda_h(t_{n+1}) \tag{9}$$

The details of this adaptive algorithm are described in a separate publication [7].

3.2. Dynamic mesh adaptation

By refinement of some basic triangulation T_h of area T current simulating mesh $\Lambda_h(t_n)$ with a fine triangulated belt area of width $\epsilon\pi$ around the void metal-interface is produced and maintained according to the conditions defined in the following sections.

3.2.1. Setting of the initial order parameter profile and initial mesh refinement $\Lambda_h(0)$

The initial order parameter profile depends on the initial shape of the void $\Gamma(0)$ and can be expressed as

$$\phi(x,y) = \begin{cases} +1 & \text{if} \quad d > \frac{\epsilon\pi}{2}, \\ \sin(\frac{d}{\epsilon}) & \text{if} \quad |d| \leq \frac{\epsilon\pi}{2}, \\ -1 & \text{if} \quad d < -\frac{\epsilon\pi}{2} \end{cases} \tag{10}$$

Where $d = dist(P(x,y), \Gamma(0))$ is the signed normal distance of the point from the initial interface $\Gamma(0)$. To sufficient resolution of this initial profile, the basic mesh T_h is transformed into mesh $\Lambda_h(0)$ obeying the following criterion:
The *initial mesh refinement criterion (IMRC)* for the circular void with center O and radius r is:

$$\forall K \in T_h \quad \text{if} \quad |dist(C_K, O) - r| \leq \frac{\epsilon\pi}{2} \quad \text{than} \quad h_K < \frac{\epsilon\pi}{n} \tag{11}$$

n is the chosen number of mesh elements across the void-metal interface width, h_K is the longest vertex of the triangle K, and C_K is its center of gravity. Now an adaptive algorithm Ψ transforms the initial mesh T_h according to $IMRC$.

$$\Psi(T_h, IMRC) = \Lambda_h(0) \tag{12}$$

This means that each element of T_h is recursively adapted by algorithm Ψ until $IMRC$ is satisfied. The initial order parameter distribution (10) is set on mesh $\Lambda_h(0)$.

3.2.2. Maintaining the mesh during simulation

After an order parameter was evaluated on the $\Lambda_h(t_{n-1})$ a mesh needs to be adapted according to the new void-metal interface position. Therefore it is necessary to extract all elements which are cut by void-metal interface in mesh $\Lambda_h(t_{n-1})$. The following condition is used: Let us take a triangle $K \in \Lambda_h(t_{n-1})$ and denote its vertices as P_0, P_1, P_2.

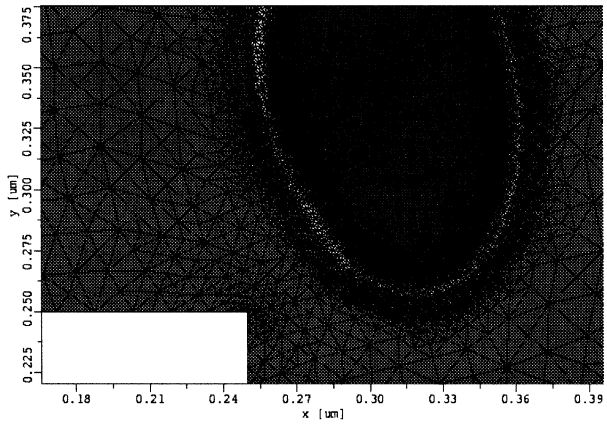

Fig. 1. Refined mesh around the void.

The triangle K belongs to the interfacial elements if for the values of order parameter ϕ at the triangle's vertices holds $\phi(P_0)\phi(P_1) < 0$ or $\phi(P_1)\phi(P_2) < 0$. We assume that an interface intersects each edge of the element only once. The set of all interfacial elements at the time t_{n-1} is denoted as $E(t_{n-1})$. The Centrex of gravity of each triangle from the $E(t_{n-1})$ build the interface point list $L(t_{n-1})$. The distance of the arbitrary point Q from $L(t_{n-1})$ is defined as

$$dist(Q, L(t_{n-1})) = \min_{P \in L(t_{n-1})} dist(Q, P). \tag{13}$$

Thus we can define the *transitional mesh refinement criterion TMRC*

$$\forall K \in T_h \quad \text{if} \quad dist(C_K, L(t_{n-1})) \leq \frac{\epsilon\pi}{2} \quad \text{than} \quad h_K < \frac{\epsilon\pi}{n} \tag{14}$$

and the mesh adapting for the next time step evaluation of parameter can be expressed as

$$\Psi(\Lambda_h(t_{n-1}), TMRC) = \Lambda_h(t_n) \tag{15}$$

$TMRC$ ensures fine mesh resolution of the belt area of width $\epsilon\pi$ around the newly evaluated void-metal interface with n elements across it (Fig. 1.).

4. Results and discussion

The calculations are completed applying the finite element discrete scheme (4)-(7) and mesh adaptation (13)-(15) sequentially. The time step Δt for the finite element scheme is fitted to the simulations begin taking into account inverse proportionality of the speed of the evolving void-metal interface to the initial void radius [6]. An appropriate choice of the time step ensures that the evolving void-metal interface will stay inside the fine mesh belt during the simulation.
Simulations have shown that the voids follow the electric current direction. In the linear part of the via voids exhibit similar shape changes as observed in the earlier diffuse interface [1, 3] and sharp interface models [6, 2] which considered linear interconnect geometry only. There is also no significant fluctuation of the resistance during this period of interconnect evolution. The situation changes when the void evolves in the proximity of an interconnect corner. Due to current crowding in this area the influence of the electromigration force on the material transport on the void surface is more pronounced than the chemical potential gradient and this unbalance leads to higher

asymmetry in the void shape then observed in the linear part of the interconnect. This shape change and the position of the void at the interconnect corner causes a characteristical profile of the resistance change which shows a lowering of the electromigration damage influence on the interconnect resistance for a time duration depending on the initial void size (Fig. 2.).

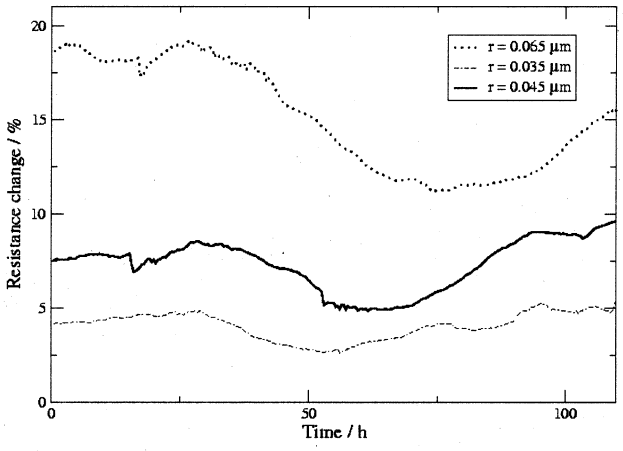

Fig. 2. Time dependent resistance change during void evolution for the different initial void radius.

It was also observed, that independent of the initial void size, voids retains their stability and do not transform in slit or wedge like formations which have been shown to be a main cause for the complete interconnect failure [8].

5. Conclusion

A governing diffuse interface equation for the order parameter coupled with the Laplace equation for the electrical field is solved using the finite element schema suited to dynamically adapted mesh. The mesh is maintained by a refinement-coarsening algorithm controlled by position, curvature and width of the simulated void-metal interface which distributes the mesh density in such a way that it allows an efficient simulation of evolving voids through large portions of a complex interconnect geometry. The presented method is well suited for long time prediction of resistance change due to electromigration during the interconnect life time.

Acknowledgment

This research project is supported by the European Community MULSIC project.

References

[1] Mahadevan M, Bradley R. Phase field model of surface electromigration in single crystal metal thin films. Physica D 1999;126: p.201-213.

[2] Rauf Gungor M, Maroudas D. Theoretical analysis of electromigration-induced failure of metallic thin films due to transgranular void propagation . J. Appl. Phys. 1999;85(4): p.2233-2246.

[3] Bhate DN, Kummar A, Bower AF. Diffuse interface model for electromigration and stress voiding. J. Appl. Phys. 2000;87(4): p.1712-1721.

[4] Blowey J, Elliott C. Weak and Variational Methods for Moving Boundary Problems. Pitman Publishing Inc., 1981.

[5] Kossacky I. A recursive approach to local mesh refinement in two and three dimensions. J. Comput. Appl. Math. 1994;55: p.275-288.

[6] Fridline DR, Bower AF. Influence of anisotropic surface diffusivity on electromigration induced void migration and evolution. J. Appl. Phys. 1999;85(6): p.3168-3174.

[7] Ceric H, Selberherr S. An adaptive grid approach for the simulation of electromigration induced void migration. SISPAD 2002

[8] Arzt E, Kraft O, Nix WD, Sanchez JE. Electromigration failure by shape change of voids in bamboo lines. J. Appl. Phys. 1994;76(3): p.1563-1571.